Available online at www.sciencedirect.com

ScienceDirect

JOURNAL OF IRON AND STEEL RESEARCH, INTERNATIONAL. 2016, 23(1): 48-52

Interactions of Shear Bands in a Ductile Metallic Glass

Li-shan HUO[1,2], Jun-qiang WANG[1,2], Jun-tao HUO[1,2], Yuan-yun ZHAO[1,2], He MEN[1,2], Chun-tao CHANG[1,2], Xin-min WANG[1,2], Run-wei LI[1,2]

(1. Key Laboratory of Magnetic Materials and Devices, Ningbo Institute of Materials Technology & Engineering, Chinese Academy of Sciences, Ningbo 315201, Zhejiang, China; 2. Zhejiang Province Key Laboratory of Magnetic Materials and Application Technology, Ningbo Institute of Materials Technology & Engineering, Chinese Academy of Sciences, Ningbo 315201, Zhejiang, China)

Abstract: Shear bands play a key role in the plastic deformation of metallic glasses (MGs). Even though there are extensive studies on the initiation and propagation of shear bands, the interactions among them have not been systematically studied yet. The interactions between the primary shear bands (PSBs) and secondary shear bands (SSBs) in a ductile Zr-based MG were studied. The residual stress near PSBs can deflect the propagation direction and reduce the propagation velocity of SSBs, which contributes to the plasticity and toughness of the MG. It was demonstrated that the probability and strength of the interactions between PSBs and SSBs would become stronger for MGs with larger Young's modulus and smaller shear modulus, i. e., larger Poisson's ratio. These results are valuable in understanding the plastic deformation of MGs and may be helpful in designing new MGs with desirable mechanical properties.

Key words: bulk metallic glass; shear band; interaction; plasticity; serration

Bulk metallic glasses (BMGs) have promising applications as the structural materials due to their superior mechanical properties, e. g., excellent elasticity, high strength and high hardness. However, the limited ductility has always been an inherent obstacle for their applications, and extensive efforts have been devoted to developing the ductile BMGs[1-3]. It has been widely recognized that their plastic deformations at temperatures far below the glass transition temperature usually occur via the formation of shear bands (SBs). The nucleation[4-8], propagation[9-14] and interaction[15,16] are three key processes for the SB operation. The nucleation of SBs derives from the activation and percolation of the flow units, also called as shear transformation zones[17,18]. The activation of flow units is a thermally activated phenomenon, whose activation energy is quite close to that of the secondary relaxations in BMGs[19]. The propagation speed of SBs can be as high as the sound velocity[20,21], which is much faster than the slip velocity of the sample on the two sides of a SB[10]. The propagation of SBs is a stress-controlled behavior. For an as-cast BMG sample, the SB propagation is usually about 45° to the uniaxial compression direction[22]. When introducing stress with directions different from that of the natural SB propagation, they will change their propagation directions, along the new maximum shear stress orientation. Various methods have been tried to introduce the residual stress to change the propagation direction of SBs, and have proved to be effective in improving the apparent plasticity of BMGs[11,13,14,23-25]. Even though there are many researches on the initiation and propagation of SBs, few is known about how they interact with each other and contribute to the plasticity during deformation[12].

In this study, the interactions of SBs in a ductile Zr-based BMG with a 17% compressive plasticity were investigated. During the plastic deformation, plenty of SBs were formed, which correspond to the

Foundation Item: Item Sponsored by China Postdoctoral Science Foundation (2014M551779); Ningbo Municipal Natural Science Foundation of China (2015A610005, 2015A610064); One Hundred Talents Program of Chinese Academy of Sciences

Biography: Li-shan HUO, Doctor, Assistant Professor; **E-mail**: huolishan@nimte.ac.cn; **Received Date**: September 10, 2015

Corresponding Author: Jun-qiang WANG, Doctor, Professor; **E-mail**: jqwang@nimte.ac.cn

Chun-tao CHANG, Doctor, Professor; **E-mail**: ctchang@nimte.ac.cn

serrations (stress drops) in the stress-strain curve. The ones formed with large stress drops can be defined as primary shear bands (PSBs), while the ones causing only small stress drops can be defined as secondary shear bands (SSBs). It was shown that SSBs usually initiated from a PSB and that their sliding directions usually got deflected when propagating in the vicinity of a PSB. A qualitative model was proposed to demonstrate the interactions among the SBs and their relations with the properties of BMGs.

1 Experimental

The master alloy with nominal composition of $Zr_{52}Cu_{18}Ni_{15}Al_{10}Ti_5$ (at. %) was prepared by melting high purity elements (>99.9 mass%) using the arc melting furnace under the protection of Ar atmosphere. Then, the master alloy was remelted in a quartz tube using an induction furnace and subsequently injected into a copper mold to form the BMG rods with 2 mm in diameter. The amorphous nature of the rods was confirmed by X-ray diffraction and differential scanning calorimetry (data not shown here). Samples in the dimension of ϕ2 mm×4 mm were used for quasi-static compression tests with a strain rate of 10^{-4} s^{-1}. The surface morphologies of the sample and SB distributions were studied using the scanning electron microscope (SEM).

2 Results and Discussion

2.1 Serration behaviors of the BMG

Fig. 1 shows the nominal compressive stress-strain curve of the BMG. After 2.1% elastic deformation, the sample exhibits 17% plasticity before fracture. The plastic strain curve at two deformation stages is magnified and shown in the insets. During the steady plastic deformation, multiple stress drops (see the left inset in Fig. 1) exist, which

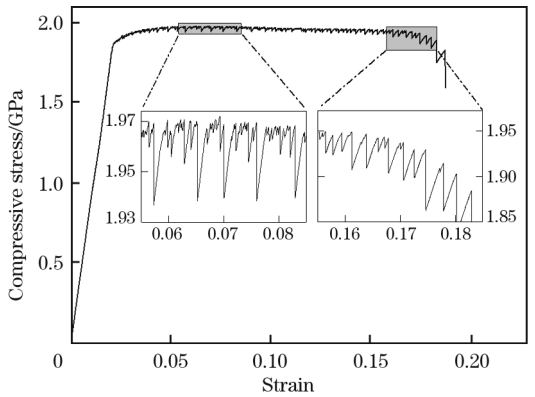

Fig. 1 Compressive stress-strain curve of BMG at strain rate of 10^{-4} s^{-1}

are attributed to the formation of multiple new SBs[7]. In this steady serration, the maximum stress drop (approximately 0.03 GPa) is about 1.6% of the yield stress (R_e=1.9 GPa). When approaching the fracture, the stress drops increase to as high as 3.4% of the yield stress, which are not stable and attributed to the stick-slip sliding movement of PSBs[26,27].

Then, the stress drops during the plastic deformation are studied statistically, as shown in Fig. 2. The stress drop versus the corresponding frequency count is plotted in Fig. 2(a), which can be well fitted by a power law relation, $y=0.0149x^{-1.41}$. This demonstrates that the plastic deformation in this alloy is a self-organized critical (SOC) state, which is quite consistent with the previously reported results in other ductile BMGs[7,28]. The emergence of the SOC state also indicates that the effect of shear band interaction on the dynamic behaviors during the deformation of MGs must be considered[7]. The normalized cumulative count versus stress drop is shown in Fig. 2(b). It can be seen that

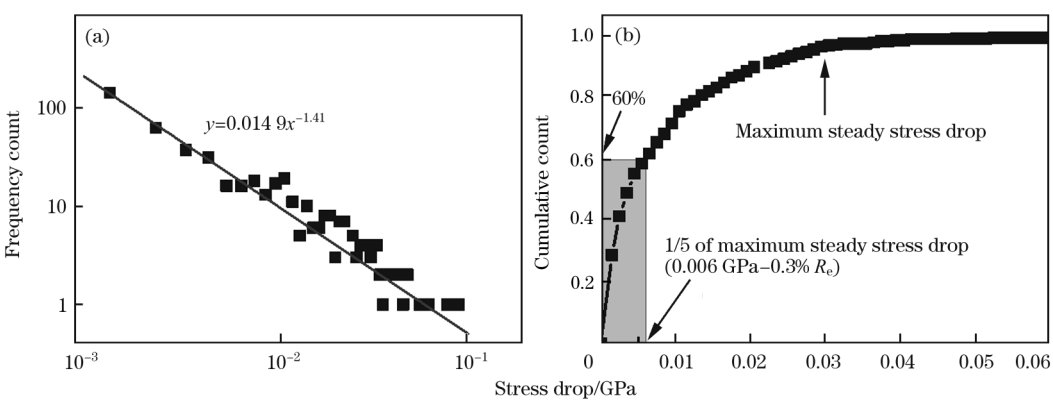

Fig. 2 Double logarithmic plot of statistical analysis of stress drop distribution at serration plastic deformation range (a) and cumulative count of stress drops during serration plastic deformation (b)

the small stress drops caused by the SSBs contribute much more, compared to the large stress drops by PSBs. Given that the maximum stress drop during the steady plastic deformation is about 0.03 GPa (see the left inset in Fig. 1), the amount of small stress drops that are lower than 0.006 GPa (1/5 of the maximum drop) is about 60% of the total drops. Thus, the formation of SSBs is very important for the plastic deformation, and it is worthy to study their propagation behaviors and interactions with the PSBs.

2.2 Interactions between PSBs and SSBs

During the uniaxial compression, the propagation direction of a SB is determined by the maximum shear stress plane, which is usually about 45° to the compression direction. The propagation of a PSB, which is accompanied by the release of large shear strain energy, usually follows the 45° behavior. However, the SSBs can change their directions when propagating close to the PSBs, due to the residual stress around the PSBs. As shown in Fig. 3(a), the SSBs initiate at PSB-1 and propagate to PSB-2, and clear deflection can be observed for a group of SSBs when they propagate approaching the pre-existed PSBs. A schematic image illustrating the interaction between the SSBs and PSBs is shown in Fig. 3(b). The darkness represents the intensity of residual stress or strain. The residual stress of the PSB has a wider distribution compared to the SSBs. When the SSBs propagate close to the PSB, the directions of SSBs deflect due to the overlapping of the PSB residual stress and external stress. The SSBs may propagate through the PSB or halt at it, because the driving energy of SSBs will be dissipated during the deflection.

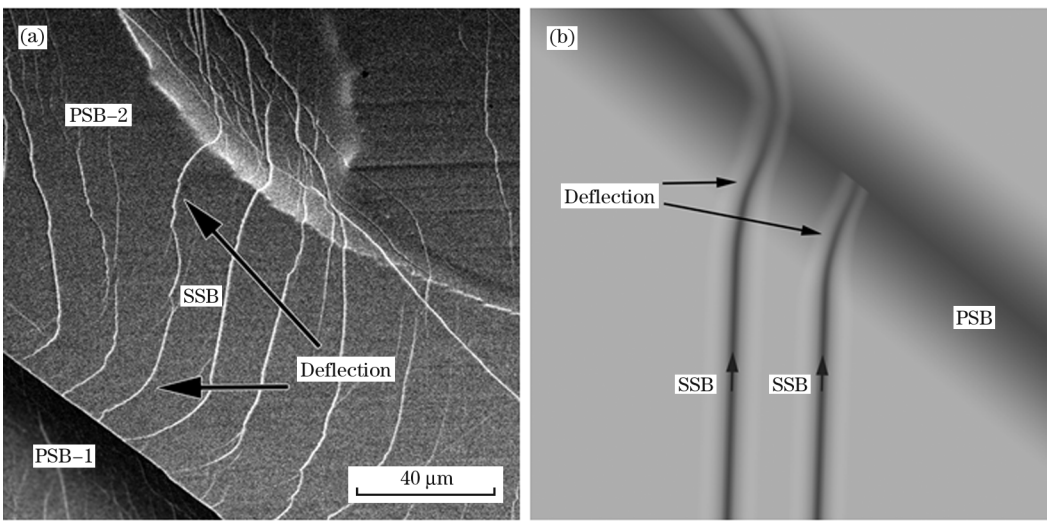

Fig. 3 SEM image of deformed sample surface composed of two PSBs and many SSBs (a) and schematic image for propagation trace of SSBs under external stress and pre-existed PSB residual stress (b)

2.3 Formation of SSBs

Fig. 4(a) exhibits part of the SB interactions after the deformation, and Fig. 4(b) gives the magnified image near position "3" in Fig. 4(a), showing the SSBs activated by the SB interactions. The black lines mark the sliding distances at different positions of the shear banding, recognized by the interruption and movement of the pre-existed SBs in Fig. 4(a), and by the shear banding steps in Fig. 4(b), respectively. The sliding distances of the shear banding are plotted versus the position of measuring sites (using "d" to represent), as shown in Figs. 4(c) and 4(d). The data can be fitted very well by linear equations with the slopes of 0.138 and 0.052, respectively. From Fig. 4(a), it can be observed that even along a PSB, the displacements at different positions are not the same, gradually decreasing from the top right to the bottom left. This is probably caused by the friction within SBs and the pinning effects from the SB interactions or material defects[12,29,30].

Based on the results shown in Figs. 4(a) and 4(c), it is proposed that the main deformation along the primary shear banding direction is compression, instead of the solely shearing. According to the phenomena displayed in Figs. 4(a) to 4(d), a sketch map is drawn to demonstrate the SB interactions and the formation of SSBs in the MG, as given in Figs. 4(e)—4(g). The PSB-1, PSB-2 and PSB-3 are all primary

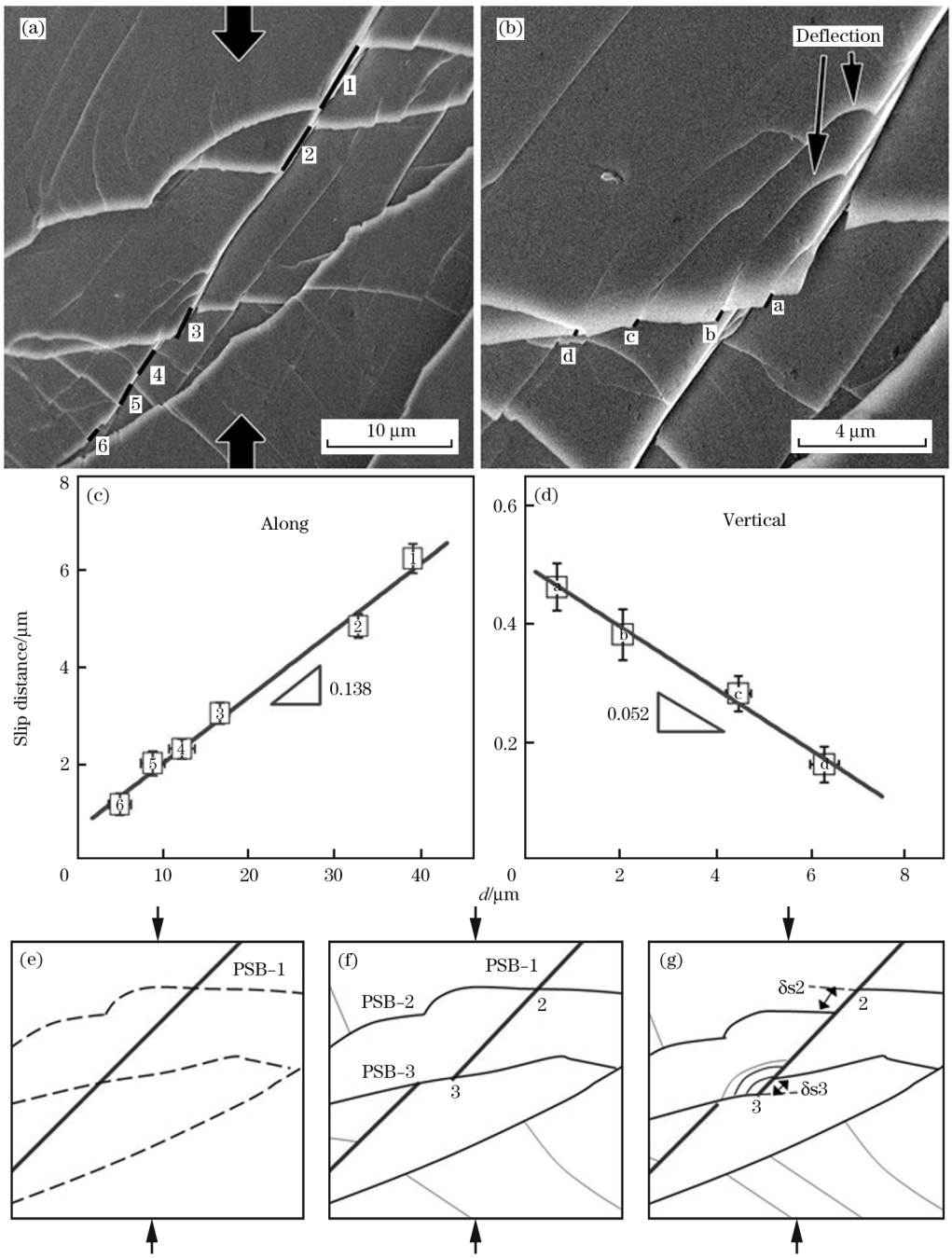

Fig. 4 SEM images of SB interactions after deformation (a, b), slip distances of different points marked in (a) versus their relative positions along the PSB (c), slip distances of the SSBs shown in (b) versus their distances (d) to the PSB (d), and sketch map illustrating the interactions of SBs near point 3 in (a) (e, f, g)

shear bands, propagating through different orientations, and the thinest lines represent the secondary shear bands. The primary shear band, PSB-1, forms at the early stage of plastic deformation. With the further deformation, other shear banding events occur, e. g. , the PSB-2 and PSB-3 (with different sliding planes and orientations from PSB-1), which interrupt the continuous shear plane of PSB-1 and yield the intersecting steps, near the positions "2" and "3". But the intersecting steps would become the barrier, impeding the further sliding of PSB-1. As the deformation continues, the strain energy stored in the alloy between two intersecting steps increases, which drives the formation and propagation of SSBs. As stated above, the main deformation along the primary shear banding direction is considered as compression. Then, the elastic strain energy density (W_E) in the alloy before the SSB formation is pro-

portional to $E\varepsilon^2$, while W_E is resulting from the compression along the shearing direction of PSB-1, E is the elastic modulus of the alloy, and ε is the compression strain along PSB-1. Since the formation and propagation of SSBs are driven by the elastic strain energy[5,18,31,32], W_E then determines the formation probability and propagation distance of SSBs. Both the formation probability and propagation distance increase with rising the W_E. Besides, the plastic shear of a material is closely related with the shear modulus G, more easily shearing with lower G[32]. Besides, the activation energy of the shear transformation zone, from which the SBs nucleate, is proportional to G[18]. Based on these discussions, it can be concluded that a larger Young′s modulus (larger driving energy) and lower shear modulus (lower resistance to SB formation), i.e., a larger Poisson′s ratio, is favorable for obtaining more SSBs and thus improved plasticity in MGs. This is consistent with previous studies[2,33]. Although the explanation stated above is derived from the results along the PSB in Figs. 4(a) and 4(b), just a tiny part of the SBs in the whole sample, it is believed to be suitable for most of the SB interactions and SSB formations, because the intersections of SBs will certainly produce the intersecting steps, which become the obstacles preventing the further sliding of pre-formed SBs and then promote the formation of new ones.

3 Conclusion

The interactions of SBs in a ductile Zr-based BMG are studied in this work. It is found that the propagation direction of SSBs can be deflected by the residual stress close to the pre-formed PSBs. Such a propagation deflection can consume the elastic energy and inhibit the further propagation, which leads to the formation of more SBs and an increase in plasticity. The interactions of SBs in the MG and the formation of SSBs are demonstrated. And from the viewpoint of SB interactions, a correlation between the plasticity and elastic moduli of MGs is found, which agrees well with previous studies. The present results can provide new insights in understanding the plastic deformation of MGs.

References:

[1] J. Schroers, W. L. Johnson, Phys. Rev. Lett. 93 (2004) 255506.

[2] Y. H. Liu, G. Wang, R. J. Wang, D. Q. Zhao, M. X. Pan, W. H. Wang, Science 315 (2007) 1385-1388.

[3] K. F. Yao, F. Ruan, Y. Q. Yang, N. Chen, Appl. Phys. Lett. 88 (2006) 122106.

[4] C. E. Packard, C. A. Schuh, Acta Mater. 55 (2007) 5348-5358.

[5] C. A. Schuh, T. C. Hufnagel, U. Ramamurty, Acta Mater. 55 (2007) 4067-4109.

[6] J. H. Perepezko, S. D. Imhoff, M. W. Chen, J. Q. Wang, S. Gonzalez, Proc. Natl. Acad. Sci. USA 111 (2014) 3938-3942.

[7] B. A. Sun, H. B. Yu, W. Jiao, H. Y. Bai, D. Q. Zhao, W. H. Wang, Phys. Rev. Lett. 105 (2010) 035501.

[8] L. Wang, Z. P. Lu, T. G. Nieh, Scripta Mater. 65 (2011) 759-762.

[9] S. X. Song, X. L. Wang, T. G. Nieh, Scripta Mater. 62 (2010) 847-850.

[10] S. X. Song, T. G. Nieh, Intermetallics 19 (2011) 1968-1977.

[11] R. T. Qu, J. X. Zhao, M. Stoica, J. Eckert, Z. F. Zhang, Mat. Sci. Eng. A 534 (2012) 365-373.

[12] R. T. Qu, Z. Q. Liu, G. Wang, Z. F. Zhang, Acta Mater. 91 (2015) 19-33.

[13] B. Sarac, J. Schroers, Nat. Commun. 4 (2013) 2158.

[14] R. T. Qu, Q. S. Zhang, Z. F. Zhang, Scripta Mater. 68 (2013) 845-848.

[15] B. A. Sun, S. Pauly, J. Tan, M. Stoica, W. H. Wang, U. Kuhn, J. Eckert, Acta Mater. 60 (2012) 4160-4171.

[16] Y. Shen, G. P. Zheng, Scripta Mater. 63 (2010) 181-184.

[17] W. H. Wang, Y. Yang, T. G. Nieh, C. T. Liu, Intermetallics 67 (2015) 81-86.

[18] W. L. Johnson, K. Samwer, Phys. Rev. Lett. 95 (2005) 195501.

[19] H. B. Yu, W. H. Wang, H. Y. Bai, Y. Wu, M. W. Chen, Phys. Rev. B 81 (2010) 220201 (R).

[20] D. Klaumünzer, A. Lazarev, R. Maaß, F. H. Dalla Torre, A. Vinogradov, J. F. Löffler, Phys. Rev. Lett. 107 (2011) 185502.

[21] J. J. Lewandowski, A. L. Greer, Nat. Mater. 5 (2006) 15-18.

[22] Z. F. Zhang, J. Eckert, L. Schultz, Acta Mater. 51 (2003) 1167-1179.

[23] Y. Zhang, W. H. Wang, A. L. Greer, Nat. Mater. 5 (2006) 857-860.

[24] H. B. Yu, J. Hu, X. X. Xia, B. A. Sun, X. X. Li, W. H. Wang, H. Y. Bai, Scripta Mater. 61 (2009) 640-643.

[25] J. L. Zhang, H. B. Yu, J. X. Lu, H. Y. Bai, C. H. Shek, Appl. Phys. Lett. 95 (2009) 071906.

[26] A. L. Greer, Y. Q. Cheng, E. Ma, Mat. Sci. Eng. R 74 (2013) 71-132.

[27] Y. Q. Cheng, Z. Han, Y. Li, E. Ma, Phys. Rev. B 80 (2009) 134115.

[28] R. Sarmah, G. Ananthakrishna, B. A. Sun, W. H. Wang, Acta Mater. 59 (2011) 4482-4493.

[29] Y. H. Liu, C. T. Liu, A. Gali, A. Inoue, M. W. Chen, Intermetallics 18 (2010)1455-1464.

[30] Y. Y. Zhao, G. Zhang, D. Estévez, C. Chang, X. Wang, R. W. Li, J. Alloys Comp. 621 (2015) 238-243.

[31] A. S. Argon, Acta Metall. 27 (1979) 47-58.

[32] Y. Wei, X. Lei, L. S. Huo, W. H. Wang, A. L. Greer, Mater. Sci. Eng. A 560 (2013) 510-517.

[33] J. J. Lewandowski, W. H. Wang, A. L. Greer, Philos. Mag. Lett. 85 (2005) 77-87.